Aerosol Delivery During High Frequency Jet Ventilation: An MRI Evaluation

Beena G Sood MD MS, Zahid Latif, Yimin Shen PhD, Robert J Galli RRT, Charles W Dunlap RRT-NPS, Matthew J Gelmini RRT, and E Mark Haacke PhD

BACKGROUND: We have previously demonstrated aerosol delivery during conventional and high frequency oscillatory (HFOV) ventilation using magnetic resonance imaging (MRI) in piglets. There are no reports on aerosol delivery during high frequency jet ventilation (HFJV). OBJECTIVE: To compare delivery of aerosolized gadopentetate dimeglumine (Gd-DTPA) in 3 neonatal ventilator circuits: conventional mechanical ventilation, HFOV, and HFJV. METHODS: Aerosols of Gd-DTPA (0.025 mol/L) generated using a jet nebulizer placed in the inspiratory limb of each ventilator were delivered into an in vitro lung model simultaneously. Multi-slice T1-weighted spin-echo sequence scans were obtained prior to and after 10 and 20 min of cumulative aerosol delivery. Gd-DTPA concentration was calculated from signal intensity changes, and the total amount of Gd-DTPA was estimated. RESULTS: Gd-DTPA was visualized in the lung model at 10 and 20 min for all 3 ventilators. Gd-DTPA delivery was highest with conventional mechanical ventilation (1.92 μmol at 10 min, 2.89 μmol at 20 min), followed by HFJV (1.59 μmol at 10 min, 1.98 μmol at 20 min) and HFOV (0.79 μmol at 10 min, 1.00 μmol at 20 min). CONCLUSIONS: This is the first report of effective aerosol delivery in a neonatal HFJV circuit. Future studies are needed for more accurate quantification of aerosol deposition. *Key words: aerosol; drug delivery; gadopentetate dimeglumine; assisted ventilation; conventional mechanical ventilation; high frequency oscillatory ventilation; high frequency jet ventilation; magnetic resonance imaging; jet nebulizer; neonatal.* [Respir Care 2012; 57(11):1901–1907. © 2012 Daedalus Enterprises]

Introduction

Neonatal hypoxemic respiratory failure in term/near-term infants is often associated with persistent pulmonary hypertension of the newborn. Aerosolized prostaglandin E_1 has been reported to be a potential selective pulmonary vasodilator.[1-3] We have previously reported the feasibility, safety, aerosol particle size distribution, and emitted dose of aerosolized prostaglandin E_1 during conventional mechanical ventilation and high frequency oscillatory ventilation (HFOV).[4-7] We have also demonstrated effective in vivo alveolar delivery of aerosolized gadopentetate dimeglumine (Gd-DTPA), a paramagnetic contrast agent, during conventional mechanical ventilation and HFOV using magnetic resonance imaging (MRI), as evaluated by signal intensity (SI) changes in the lungs and kidneys in neonatal pigs.[8,9] Critically ill neonates with neonatal hypoxemic respiratory failure may receive assisted ventilation with high frequency jet ventilation (HFJV) as an alternative to

Dr Sood is affiliated with the Department of Pediatrics; Mr Latif and Dr Shen are affiliated with the Department of Radiology; Mr Galli, Mr Dunlap, and Mr Gelmini are affiliated with the Department of Respiratory Care; Dr Sood, Mr Galli, and Mr Dunlap are also affiliated with the Children's Hospital of Michigan; Mr Dunlap is also affiliated with the Hutzel Women's Hospital; and Mr Latif, Dr Shen, and Dr Haacke are affiliated with the MR Research Facility, Wayne State University, Detroit, Michigan.

This research was partly supported by the Children's Research Center of Michigan. The authors have disclosed no conflicts of interest.

Dr Sood presented a version of this paper at the meeting of the Pediatric Academic Societies, held April 30 through May 3, 2011, in Denver, Colorado.

Correspondence: Beena G Sood MD MSc, Department of Pediatrics, Children's Hospital of Michigan, 3901 Beaubien Boulevard, 4H42, Detroit MI 48201. E-mail: bsood@med.wayne.edu.

DOI: 10.4187/respcare.01746

conventional mechanical ventilation or HFOV. Although aerosols would be expected to be delivered in the presence of flow in the ventilator circuit,[10] it is generally believed that aerosols cannot be delivered during HFJV (unpublished expert opinion of neonatologists), and this has not been rigorously investigated. The present study is an extension of our previous work and was designed to assess aerosol delivery during HFJV.

Pulmonary aerosol deposition has been evaluated by theoretical in vitro models, pharmacokinetic studies, and pulmonary imaging (gamma scintigraphy, single photon emission computed tomography, positron emission tomography, and MRI) in animals and humans.[11-18] Based on our previous studies on MRI evaluation of aerosol delivery in intubated piglets, the time course of SI changes in kidneys is similar during conventional mechanical ventilation and HFOV. Thus, demonstration of aerosol delivery at the endotracheal tube (ETT) attached to an HFJV setup would suggest a similar fate in vivo, without the need for an animal model, in accordance with the Applied Research Ethics National Association/Office of Laboratory Animal Welfare Institutional Animal Care and Use Committee Guidebook recommendations. Use of MRI would provide a rapid, sensitive, and quantitative method for evaluation of aerosol delivery, with high spatial and temporal resolution, and without the use of ionizing radiation. The present study was designed to assess whether aerosolized Gd-DTPA is delivered during HFJV (qualitative assessment) and its comparison with aerosol delivery during conventional mechanical ventilation and HFOV (quantitative assessment) under identical in vitro experimental conditions, using MRI of a lung phantom model.

QUICK LOOK

Current knowledge

A myriad of factors impact aerosol delivery during mechanical ventilation. The use of high-frequency ventilation with rapid flows and frequencies can further complicate aerosol delivery. Aerosol delivery during high-frequency jet ventilation has not been well characterized.

What this paper contributes to our knowledge

Using a neonatal lung analogue, effective aerosol delivery during high-frequency jet ventilation can be accomplished. Aerosol delivery during high-frequency jet ventilation was lower than conventional ventilation but higher than high-frequency oscillatory ventilation.

Methods

Mechanical Ventilation

Conventional mechanical ventilation was initiated with a ventilator system (840, Puritan Bennett, Pleasanton, California) at a breath rate of 40 breaths/min, F_{IO_2} of 1.0, peak inspiratory pressure of 22 cm H_2O, PEEP of 5 cm H_2O, and duty cycle of 35%, to simulate clinical use in moderate to severe neonatal hypoxemic respiratory failure. HFOV was initiated with the ventilator (SensorMedics 3100A, Viasys Healthcare, Palm Springs, California) at a mean airway pressure of 16 cm H_2O, amplitude of 40 cm H_2O, frequency of 10 Hz, and duty cycle of 33%. The HFJV circuit (Bunnell, Salt Lake City, Utah) included the jet interrupter operating at a peak inspiratory pressure of 20 cm H_2O, ΔP of 15 cm H_2O, PEEP of 5 cm H_2O, and rate of 420 breaths/min, with a conventional mechanical ventilation backup rate of 6 breaths/min. A 3.5 mm inner-diameter ETT was connected to each ventilator system. The ventilator settings chosen for the 3 ventilators are the typical settings to be used in a neonate undergoing assisted ventilation. The mean airway pressures during the 3 modes of ventilation were: conventional mechanical ventilation 17 cm H_2O, HFOV 16 cm H_2O, and HFJV 10.3 cm H_2O.

In Vitro Phantom Lung Model

ETTs from each ventilator were placed in a sponge that served as a lung phantom (Ocelo, 3M, St Paul, Minnesota, 119 × 75 × 15 mm). Each ventilator circuit was set up as it would have been in clinical practice, by using the short self-test (with the 840) included in the manufacturer's software, patient circuit calibration procedure (HFOV), and visual inspection to check for airtightness. However, exhaled tidal volume could not be measured with the 840 as a sponge was being ventilated. Each sponge was moistened with 40 mL tap water at the start of the experiment. No further water was added to the sponge during the experiment. The phantom was scanned in a 3T scanner prior to aerosol delivery and after 10 and 20 min of cumulative aerosol delivery.

Preliminary experiments performed with a separate sponge for each ventilator (Fig. 1) provided an estimate of the diameter of the area of aerosol deposition after 20 min (Fig. 2). It also became clear that for results of experiments with different ventilators to be comparable, the amount of water in each sponge, and circuit humidity should be identical, as MRI signal intensity is determined by the concentration of H+ ions. Therefore, we repeated the experiments with all 3 ETTs from the 3 ventilators delivering aerosol to a single sponge (Fig. 3) on a single day. Any substantial leakage of aerosol delivered from one ventilator to another at the ETT end was ruled out by placing the ETTs at a sufficient distance apart, based on our preliminary experiments; placing the ETTs at different depths

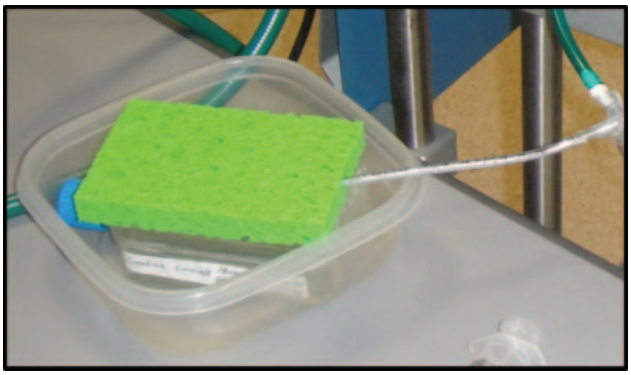

Fig. 1. An endotracheal tube connected to a jet ventilator circuit placed in a single sponge.

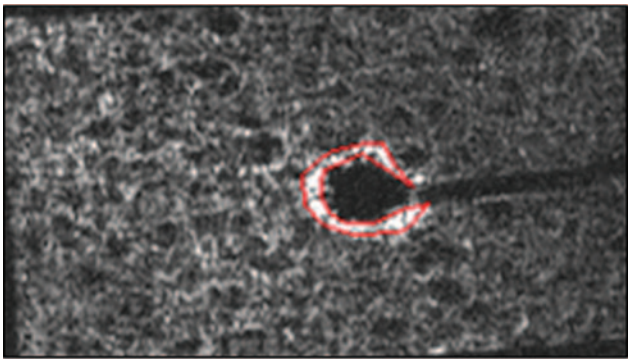

Fig. 2. Signal intensity changes around the end of the endotracheal tube in the sponge in Figure 1 in a single slice on MR imaging following aerosol administration for 20 min. The red outline marks the region of interest.

into the sponge (Fig. 4); lack of greater SI at periphery of region of interest, compared to center for each ETT (Fig. 5); lack of MRI signal connecting outputs of any 2 ventilators.

Administration of Continuous Aerosol

Aerosols of Gd-DTPA were generated with a jet nebulizer (low flow, MiniHeart, Westmed, Tucson, Arizona) driven by oxygen at a flow of 2 L/min. Three different nebulizers from the same lot were used for the 3 ventilator circuits. The low flow MiniHeart nebulizer has an output rate of 8 mL/h. The nebulizer was placed in the inspiratory limb of the clinically used neonatal ventilator circuit, where there was a natural break in the circuit, ~50 cm from the ETT for conventional mechanical ventilation and HFJV, and ~35 cm from the ETT for HFV. Aerosolization of Gd-DTPA, a para-magnetic contrast agent, was initiated after baseline MR images had been obtained without aerosol administration. At the start of aerosol therapy the nebulizer chamber in each ventilator circuit was filled with 20 mL of Gd-DTPA (0.5 mol/L) diluted in normal saline

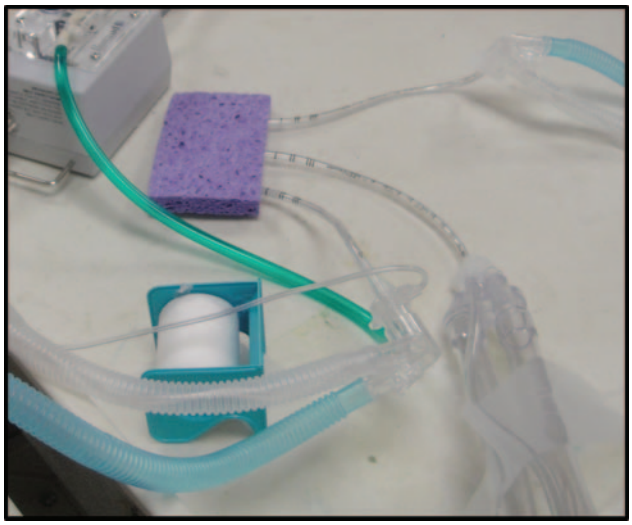

Fig. 3. Endotracheal tubes from 3 ventilator circuits (conventional mechanical ventilation, high frequency oscillatory ventilation, and high frequency jet ventilation) leading to a single sponge. The endotracheal tubes are marked with clear tape to indicate the ventilator they are connected to during aerosol administration.

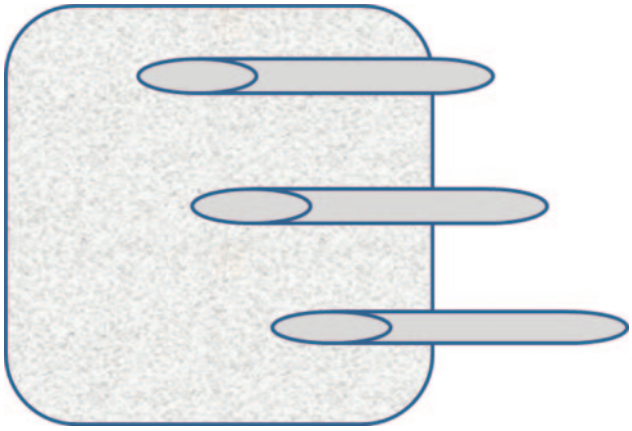

Fig. 4. Cartoon showing placement of 3 identical endotracheal tubes in a single sponge. The endotracheal tubes are placed at sufficient distance apart based on findings of Figure 2 and to a different depth inside the sponge, to avoid leakage of aerosol delivered from one ventilator to the other at the endotracheal tube end.

to yield a final concentration of 0.025 mol/L. Subsequent MRI scans were obtained after 10 min and 20 min of cumulative aerosol delivery. The time points were chosen based on our previous experiments of MR evaluation of aerosol delivery in neonatal pigs. Since MR-compatible conventional mechanical ventilation, HFOV, and HFJV were not available, the sponge was moved out of the scanner between baseline, 10 min, and 20 min scans. The ventilators were placed in a room ~4.6 m away from the MR suite. At the end of 10 min aerosol administration, the

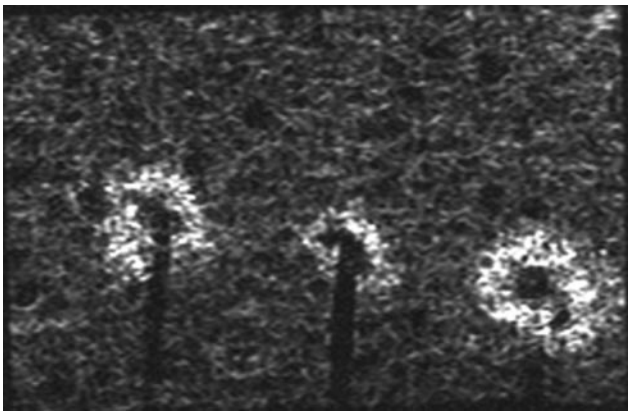

Fig. 5. Magnetic resonance imaging (MRI) of a single slice of the sponge in Figure 4, obtained after 20 min of aerosol administration. The lack of greater signal intensity at the periphery of the region of interest, compared to the center, for each endotracheal tube, and lack of MRI signal connecting outputs of any 2 ventilators rules out substantial leakage of aerosol delivered from one ventilator to another at the ETT end.

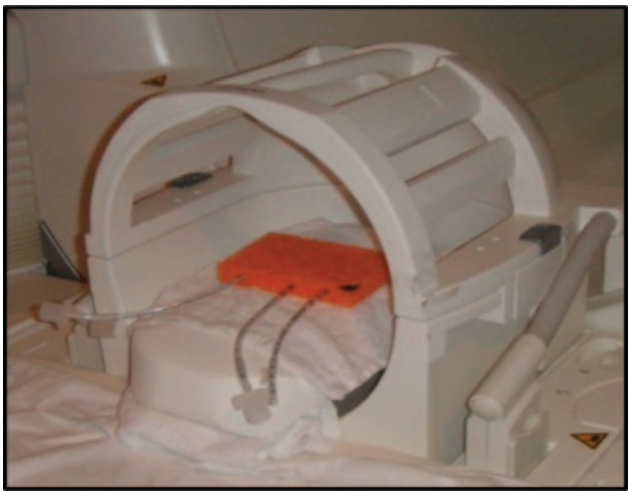

Fig. 6. A single sponge with 3 endotracheal tubes placed in a 12 channel head coil for magnetic resonance imaging. A black mark at the right upper corner of the sponge ensures consistent placement between scans; the endotracheal tubes are marked with clear tape to indicate the ventilator they are connected to during aerosol administration.

sponge was transported to the MR suite: this took 30 seconds. The sponge was then scanned for 15 min and returned to the ventilators for another 10 min of aerosol delivery.

Magnetic Resonance Imaging

The sponges were scanned in a 3T MR scanner (Magnetom Verio 3T, Siemens, Berlin, Germany), using a multislice T1 weighted spin-echo sequence with a 12 channel head coil (Fig. 6). Imaging parameters included: TR/TE = 294/15 ms, BW = 203 Hz/px. FOV = 200 × 200 mm^2, matrix size = 384 × 69, interpolated to 384 × 384, in-plane resolution = 0.528 × 0.528 mm^2, 11 slices, 3 mm in thickness, with 10% gap, Voxel volume = 0.814 mm^3, one average, acquisition time (TA) 2 min, 42 s. A FLASH sequence with multiple flip angles was used for T1 measurement, with TR/TE = 54/2.18 ms, FA = 10°, 20°, 30°, and 40°, pixel bandwidth = 400 Hz, resolution = 3.35 × 2.34 × 5, interpolated to 2.34 × 2.34 × 5 mm^3, and TA = 2 min, 36 s for each flip angle. Scan time was 15 min.

SI changes in regions of interest surrounding the end of the ETT from each ventilator were used to calculate Gd concentration as described previously.[8] Concentration of Gd was extracted from the ratio of the SI as a function of time, s(t), to the signal intensity at baseline, s(0). SI as a function of time is proportional to (1 – exp (–TR/T1 (t)). The ratio s(t)/s(0) can be calculated directly. To convert this ratio to concentration requires a knowledge of T1(0) in the equation $1/T1(t) = 1/T1(0) + \alpha.c(t)$, where α is approximately 5 mM/s, c(t) is the concentration of Gd as a function of time, and T1(t) is calculated from $T1(t) = -TR/\ln\{1 - [1 - \exp(-TR/T1(0))]s(t)/s(0)\}$ from the spin echo data. An average T1(0) extracted over all pixels with enhanced SI in the sponge was used. The total amount of Gd-DTPA deposited was calculated from the product of Gd concentration and total volume. Total volume of the regions of interest was calculated as the product of pixel volume and number of pixels. Gd concentration was extracted from enhanced SIs in the regions of interest in each slice and summed over all slices for each ventilator. Delivered dose to the sponge was calculated as percent Gd deposited on sponge, assuming a nebulizer output of 8 mL/h.

MR images were analyzed using our internally developed signal processing software (MR SPIN in NMR), which is written in Visual C++ for the Windows platform (http://www.mrc.wayne.edu/) (Windows, Microsoft, Redmond, Washington). Statistical analysis was performed using SAS statistics software (PROC GLM in SAS 19.2, SAS Institute, Cary, North Carolina).

Results

Contrast was visualized in the lung mimicking phantom at 10 and 20 min for all 3 ventilators (Fig. 7). Consistent data were obtained in 3 repetitions of the experiments under identical conditions. Mean Gd delivery (μmol) was highest with conventional mechanical ventilation (1.92 μmol at 10 min, 2.89 μmol at 20 min) followed by HFJV (1.59 μmol at 10 min, 1.98 μmol at 20 min) and HFOV (0.79 μmol at 10 min, 1.00 μmol at 20 min) (Fig. 8). There was a significant increase in Gd deposited over time

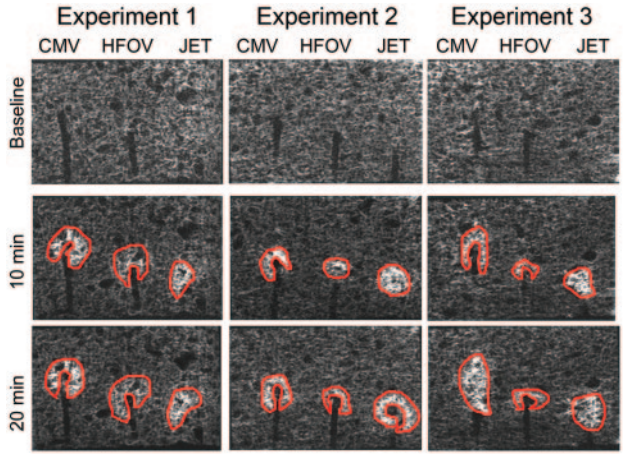

Fig. 7. This figure shows MR images obtained at baseline and at 10 and 20 min after cumulative aerosol administration in 3 series of experiments. Each image represents a single slice; to ensure that the same slices were sampled at the 3 time points, the sponge was placed in the scanner in exactly the same position at the 3 time points. In each experiment, aerosols from conventional mechanical ventilation, HFOV and HFJV were administered simultaneously in a single sponge, which served as a lung model. The top panel represents images obtained at baseline. Gadopentetate dimeglumine (Gd-DTPA) is visualized in post-aerosol images at both 10 and 20 min with all ventilators and in all experiments.

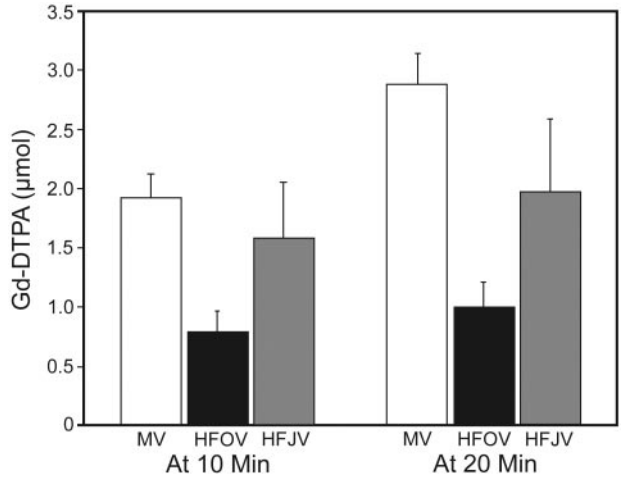

Fig. 8. Total amount of gadopentetate dimeglumine (Gd-DTPA) (μmol) delivered at 10 and 20 min for each ventilator type. Total Gd-DTPA was calculated from changes in signal intensity. The error bars represent one standard error.

($P < .001$) and a significant interaction between time and ventilation mode ($P = .002$). Delivered dose, calculated as percent Gd deposited on the sponge, assuming a nebulizer output of 8 mL/h, was highest for conventional mechanical ventilation (5.8% at 10 min and 4.3% at 20 min), followed by HFJV (4.8% at 10 min and 3.0% at 20 min) and HFOV (2.4% at 10 min and 1.5% at 20 min).

Discussion

This study describes for the first time effective in vitro aerosol delivery in a neonatal HFJV circuit, using MRI of an innovative and inexpensive lung phantom, by comparison with delivery during conventional mechanical ventilation and HFOV, which we have previously validated in a piglet model. We have shown statistically significant aerosol delivery over time for conventional mechanical ventilation, HFOV, and HFJV and an interaction with ventilator mode. Aerosol deposition in the HFJV circuit was intermediate between that observed with conventional mechanical ventilation and HFOV under identical experimental conditions. The absolute estimated delivered dose was most likely an underestimate; however, the relative delivered dose in the 3 neonatal ventilator circuits is probably a true reflection of differences in aerosol delivery in these ventilator systems. Although there was an increase in delivered dose between the 10 min and 20 min scans, the increase was not linear. This could be a result of constant efflux of aerosol deposited over time, non-linear relationship between Gd concentration and SI changes, and decrease in Gd concentration gradient in the sponge over time. The results of this study need to be validated in longer term experiments using different lung models.

A complex array of factors influence aerosol delivery during mechanical ventilation, including variables related to the nebulizer, aerosol particle size, the ventilator circuit and artificial airway, the inhaled drug or agent, the patient/model, and the evaluation technique.[12,19,20] Aerosol deposition has been evaluated by theoretical in vitro models, pharmacokinetic studies, and pulmonary imaging (gamma scintigraphy, single photon emission computed tomography, positron emission tomography, and MRI) in animals and humans.[11-18] In this report we have used MRI to evaluate deposition of aerosolized Gd-DTPA, a paramagnetic contrast agent, in an innovative, inexpensive lung phantom. Physicochemical properties and aerosol particle size have been previously characterized for Gd-DTPA, with 50% of particles being smaller than 2.5 μm.[21] We have previously reported the aerosol particle size distribution of prostaglandin E_1 using the MiniHeart nebulizer.[6] The aerosol particle size for both prostaglandin E_1 and Gd-DTPA favors alveolar deposition.

The time course of MR visualization of Gd-DTPA in the lung phantom was similar to that reported during conventional mechanical ventilation.[8] Delivered dose to the sponge was calculated as percent Gd deposited on the sponge, assuming a nebulizer output of 8 mL/h, as has been reported by the manufacturer. Since the nebulizer device used in these experiments is FDA approved,[22] widely used clinically, with demonstrated effectiveness in previous publications,[4-6,8,9,23-28] we did not repeat experiments to validate nebulizer output. Delivered dose was calculated

as a percent of known nebulizer output (8 mL/h) rather than volume of Gd placed in the nebulizer (20 mL), which greatly exceeded the nebulizer output. Calculating Gd deposited as a percentage of the volume placed in the nebulizer chamber would introduce an error, as the percentage would vary, depending on the amount placed in the nebulizer, as long as this exceeded the nebulizer's output.

The delivered dose in this report is lower than that reported in adult (57–81%) but higher than that reported in pediatric ventilation studies (0.2–10%).[29-36] In an in vitro wet lung model involving chemical analysis of prostaglandin E_1, we had previously demonstrated an emitted dose of 32–40% following conventional mechanical ventilation and 0.1% following HFOV.[6] Recently, Davies et al reported lack of deposition in ex vivo pig lungs of aerosols of technetium labeled DTPA generated by a vibrating mesh nebulizer placed in the conventional mechanical ventilation circuit of a HFJV setup ($n = 2$). However, placement of the vibrating mesh nebulizer in the jet interrupter system of the HFJV circuit ($n = 2$) greatly enhanced central airway delivery, although parenchymal delivery remained very low.[37] These discrepancies in results of aerosol deposition studies are probably related to differences in ventilator systems, nebulizer design, lung model, and assessment techniques.[38]

Despite the important findings described in this study, there are potential deficiencies. Limitations of our study include the inability of our lung phantom to mimic the complex anatomy of the neonatal respiratory system, and the effect of disease state on aerosol drug delivery. The variability in the air pockets in the sponge may have introduced an error in the quantification of aerosol deposited, thus underestimating the actual amount of aerosol deposited. Another factor that contributed to underestimation of aerosol delivered was the inability to take into account the Gd deposited in the gap between scanned slices. Since HFOV and HFJV are not MR compatible, the sponge had to be moved between scans obtained at baseline, 10 min, and 20 min, thus introducing another source of error in the quantification of Gd concentration. To minimize this error, every attempt was made to replace the sponge in the scanner in exactly the same position.

Other factors that may have contributed to errors in estimation of percent Gd delivered include the use of T1 averaged over the entire sponge, instead of voxel-specific T1 for calculating Gd concentration, changes in water concentration in the sponge over time, and assumption of constant nebulizer output of 8 mL/h. However, since all ventilators were tested in identical experimental conditions using a single sponge, although the absolute estimates of Gd delivered may be underestimated, the relative estimates of Gd delivered are likely accurate. Finally, we did not investigate the effect of other ventilator-related factors such as circuit flow and humidity on aerosol delivery. The effects of these factors on aerosol delivery have been reported before; the primary goal of this study was to validate that aerosol is delivered in a HFJV circuit, by comparison with delivery during conventional mechanical ventilation and HFOV, which we have previously validated in a piglet model.

Conclusions

In conclusion, we have successfully demonstrated effective aerosol delivery in a neonatal HFJV circuit using MRI of an inexpensive lung phantom. Aerosol deposition in the neonatal HFJV circuit was intermediate between that observed in neonatal conventional mechanical ventilation and HFOV circuits. The absolute estimated delivered dose was most likely an underestimate; however, the relative delivered dose in the 3 neonatal ventilator circuits is probably a true reflection of differences in aerosol delivery in these ventilator systems. Future studies are needed for more accurate quantification of delivered dose during conventional mechanical ventilation, HFOV, and HFJV, taking into account nebulizer-, ventilator-, and patient/model-related factors. The use of a closed system lung model, more sensitive MRI techniques and MR-compatible equipment may allow earlier detection of contrast and more accurate quantification of delivered dose following administration of aerosol. MR imaging using T1 enhancing contrast agents such as Gd-DTPA may be a powerful noninvasive, real-time technique, not only for comparing aerosol delivery from different aerosol devices and ventilator circuits, but, more importantly, in understanding spatial and temporal drug distribution and disposition in vivo in animal and human models in the presence and absence of lung disease.

ACKNOWLEDGMENTS

We gratefully acknowledge the assistance of Barbara Maynarich, Information Resources Technician, and Cathy Eames MSLS in searching the medical literature and preparing the bibliography.

REFERENCES

1. Walmrath D, Schermuly R, Pilch J, Grimminger F, Seeger W. Effects of inhaled versus intravenous vasodilators in experimental pulmonary hypertension. Eur Respir J 1997;10(5):1084-2092.
2. Meyer J, Theilmeier G, Van Aken H, Bone HG, Busse H, Waurick R, et al. Inhaled prostaglandin E1 for treatment of acute lung injury in severe multiple organ failure. Anesth Analg 1998;86(4):753-758.
3. Putensen C, Hormann C, Kleinsasser A, Putensen-Himmer G. Cardiopulmonary effects of aerosolized prostaglandin E1 and nitric oxide inhalation in patients with acute respiratory distress syndrome. Am J Respir Crit Care Med 1998;157(6 Pt 1):1743-1747.
4. Sood BG, Delaney-Black V, Aranda JV, Shankaran S. Aerosolized PGE_1: a selective pulmonary vasodilator in neonatal hypoxemic respiratory failure results of a phase I/II open label clinical trial. Pediatr Res 2004;56(4):579-585.

5. Sood BG, Glibetic M, Aranda JV, Delaney-Black V, Chen X, Shankaran S. Systemic levels following PGE1 inhalation in neonatal hypoxemic respiratory failure. Acta Paediatr 2006;95(9):1093-1098.
6. Sood BG, Peterson J, Malian M, Galli R, Geisor-Walter M, McKinnon J, et al. Jet nebulization of prostaglandin E1 during neonatal mechanical ventilation: stability, emitted dose and aerosol particle size. Pharmacol Res 2007;56(6):531-541.
7. Sood BG, Dawe EJ, Rao Maddipati K, Malian M, Chen X, Galli R, et al. Toxicity of prolonged high dose inhaled PGE1 in ventilated neonatal pigs. Pulm Pharmacol Ther 2008;21(3):565-572.
8. Sood BG, Shen Y, Latif Z, Chen X, Sharp J, Neelavalli J, et al. Aerosol delivery in ventilated newborn pigs: an MRI evaluation. Pediatr Res 2008;64(2):159-164.
9. Sood BG, Shen Y, Latif Z, Galli R, Dawe EJ, Haacke EM. MRI validation of aerosol delivery during high frequency ventilation in neonatal pigs. Respirology 2010;15(3):551-555.
10. Mazela J, Polin RA. Aerosol delivery to ventilated newborn infants: historical challenges and new directions. Eur J Pediatr 2011;170(4):433-444.
11. O'Riordan TG, Palmer LB, Smaldone GC. Aerosol deposition in mechanically ventilated patients. Optimizing nebulizer delivery. Am J Respir Crit Care Med 1994;149(1):214-219.
12. Dhand R. Basic techniques for aerosol delivery during mechanical ventilation. Respir Care 2004;49(6):611-622.
13. Stuart BO. Deposition of inhaled aerosols. Arch Intern Med 1973;131(1):60-73.
14. Newman SP, Wilding IR. Imaging techniques for assessing drug delivery in man. Pharm Sci Technol Today 1999;2(5):181-189.
15. Kim CS. Methods of calculating lung delivery and deposition of aerosol particles. Respir Care 2000;45(6):695-711.
16. Sangwan S, Condos R, Smaldone GC. Lung deposition and respirable mass during wet nebulization. J Aerosol Med 2003;16(4):379-386.
17. Dubus JC, Vecellio L, De Monte M, Fink JB, Grimbert D, Montharu J, et al. Aerosol deposition in neonatal ventilation. Pediatr Res 2005;58(1):10-14.
18. Finlay WH, Stapleton KW, Chan HK, Zuberbuhler P, Gonda I. Regional deposition of inhaled hygroscopic aerosols: in vivo SPECT compared with mathematical modeling. J Appl Physiol 1996;81(1):374-383.
19. Alternative routes of drug administration: advantages and disadvantages (subject review). American Academy of Pediatrics. Committee on Drugs. Pediatrics 1997;100(1):143-152.
20. Ari A, Atalay OT, Harwood R, Sheard MM, Aljamhan EA, Fink JB. Influence of nebulizer type, position, and bias flow on aerosol drug delivery in simulated pediatric and adult lung models during mechanical ventilation. Respir Care 2010;55(7):845-851.
21. Misselwitz B, Muhler A, Heinzelmann I, Bock JC, Weinmann HJ. Magnetic resonance imaging of pulmonary ventilation. Initial experiences with a gadolinium-DTPA-based aerosol. Invest Radiol 1997;32(12):797-801.
22. Vortran Medical Technology MiniNEB 510(k) submission to the Food and Drug Administration, Center for Device and Radiological Health, Office of Device Evaluation. 1992.
23. Ferrante S, Painter E. Continuous nebulization: a treatment modality for pediatric asthma patients. Pediatr Nurs 1995;21(4):327-331.
24. Dijk PH, Heikamp A, Bambang Oetomo S. Surfactant nebulisation: lung function, surfactant distribution and pulmonary blood flow distribution in lung lavaged rabbits. Intensive Care Med 1997;23(10):1070-1076.
25. Brown B, Harwood B. An in vitro comparison of two methods of aerosolized bronchodilator delivery to intubated mechanically ventilated neonates (abstract). Respir Care 1998;43(10):844.
26. Cheney S, Crezee K, Macknight T, Wright J. Comparing pressure changes and aerosol deposition of a standard small-volume nebulizer and a Mini-HEART low flow nebulizer during HFOV (abstract). Respir Care 2009;54(11):1524.
27. Sood BG, Chen X, Dawe EJ, Malian M, Maddipati KR. Tissue distribution, metabolism and excretion of PGE1 following prolonged high-dose inhalation in neonatal pigs. Int J Pharmacol 2010;6(3):224-230.
28. Lewis J, Ikegami M, Higuchi R, Jobe A, Absolom D. Nebulized vs instilled exogenous surfactant in an adult lung injury model. J Appl Physiol 1991;71(4):1270-1276.
29. Siobal MS, Kallet RH, Pittet JF, Warnecke EL, Kraemer RW, Venkayya RV, et al. Description and evaluation of a delivery system for aerosolized prostacyclin. Respir Care 2003;48(8):742-753.
30. Coleman DM, Kelly HW, McWilliams BC. Determinants of aerosolized albuterol delivery to mechanically ventilated infants. Chest 1996;109(6):1607-1613.
31. Di Paolo ER, Pannatier A, Cotting J. In vitro evaluation of bronchodilator drug delivery by jet nebulization during pediatric mechanical ventilation. Pediatr Crit Care Med 2005;6(4):462-469.
32. Dijk PH, Heikamp A, Piers DA, Weller E, Bambang Oetomo S. Surfactant nebulisation: safety, efficiency and influence on surface lowering properties and biochemical composition. Intensive Care Med 1997;23(4):456-462.
33. McPeck M, Tandon R, Hughes K, Smaldone GC. Aerosol delivery during continuous nebulization. Chest 1997;111(5):1200-1205.
34. Pelkonen AS, Nikander K, Turpeinen M. Jet nebulization of budesonide suspension into a neonatal ventilator circuit: synchronized versus continuous nebulizer flow. Pediatr Pulmonol 1997;24(4):282-286.
35. Fok TF, Monkman S, Dolovich M, Gray S, Coates G, Paes B, et al. Efficiency of aerosol medication delivery from a metered dose inhaler versus jet nebulizer in infants with bronchopulmonary dysplasia. Pediatr Pulmonol 1996;21(5):301-309.
36. Dolovich MB, Millar D, Sterling L, Rhem R, Bosco AP, Kirpalani H. Lung deposition of QVAR (HFA134A-BDP) in newborn infants with bronchopulmonary dysplasia (BPD). Chest 2005;128;4(Suppl):351S.
37. Davies J, Williford L, Bartle R, Stallings R, Pagnanelli R, MacIntyre N. Aerosol delivery during high frequency oscillatory and jet ventilation (abstract). Respir Care 2011;56(11):1700.
38. Fink JB, Dhand R, Grychowski J, Fahey PJ, Tobin MJ. Reconciling in vitro and in vivo measurements of aerosol delivery from a metered-dose inhaler during mechanical ventilation and defining efficiency-enhancing factors. Am J Respir Crit Care Med 1999;159(1):63-68.